CONF-800804--26

AN EXPERIMENTAL INVESTIGATION OF A FLOW MONITORING INSTRUMENT IN AN UPPER PLENUM OF AN AIR-WATER REFLOOD TEST FACILITY*

S. K. Combs J. E. Hardy

Oak Ridge National Laboratory
Oak Ridge, Tennessee 37830

*Research sponsored by Office of Nuclear Regulatory Research, U.S. Nuclear Regulatory Commission under Interagency Agreements DOE 40-551-75 and 40-552-75 with the U.S. Department of Energy under contract W-7405-eng-26 with the Union Carbide Corporation.

ABSTRACT

Instrumentation was developed for measuring fluid phenomena in the upper plenum of pressurized water reactor reflood facilities. In particular, the instrumentation measured two-phase flow velocity and void fraction. The principle of operation of the instrumentation scheme was based on the measurement of electrical impedance. The technique of analysis of random signals from two spatially separated impedance sensors was employed to measure two-phase flow velocity. A relative admittance technique was used to determine void fraction. The performance of the instrumentation was studied in an air-water test facility. The test vessel simulated a portion of the upper plenum region of a pressurized water reactor. A turbo-probe and a gamma densitometer located inside the test vessel allowed for a comparison of velocity and void fraction data from the string probe. Void measurements from the string probe showed good agreement with gamma densitometer results over the entire testing span. Flow velocities determined by the string probe instrumentation yielded reasonable agreement when compared to turbo-probe velocities.

INTRODUCTION

Programs under the sponsorship of the U.S. Nuclear Regulatory Commission (USNRC) were initiated at the Oak Ridge National Laboratory (ORNL) to develop instrumentation for application in pressurized water reactor (PWR) safety experimental facilities. The experimental facilities are being built by Japan and West Germany. Kraftwerk Union (KWU), a German reactor vendor, is building the Upper Plenum Test Facility (UPTF) that is a full-scale model of the upper plenum region of a PWR.

In order to measure two-phase flow phenomena at the upper core support plate (UCSP) and surrounding upper plenum areas, ORNL is developing instrumentation packages to measure void fraction, two-phase flow velocity and mass flow rate. Much work has been done in the area of two-phase flow measurement; however, most has dealt with flow in pipes.[1-6] Measurements in the upper plenum region will be very geometry dependent, thus an air-water test facility was fabricated at ORNL that simulated the core-upper plenum interface area and upper plenum region.

The ORNL-developed instrumentation package consisted of a two-level sensor located in the flow field and signal conditioning electronics. The sensor design was similar to that employed by Carrard and Ledwidge[7] whose probe measured low void fractions ($\alpha < 0.25$). The string sensor in this study was designed to measure void fractions from 0 to 1.0 and two-phase flow velocities from 1 to 30 m/s (3.0 to 100 ft/s).

EXPERIMENTAL FACILITY AND PROCEDURE

A flow schematic of the test facility is shown in Fig. 1. Air and water flow rate capabilities were sized to simulate a range of flows predicted for refill and reflood conditions. As indicated in Fig. 1, the loop piping allowed water injection into the test vessel at either the hot leg or core location (or at both simultaneously). Air and the core spray water entered the bottom of the test vessel through three air-water mixers which individually fed each module of the test vessel. The capacity of the air supply was 1.5 m^3/s (3200 scfm); maximum water flow rates were 0.0076 m^3/s (120 gpm) [0.0025 m^3/s (40 gpm) per module] for both the core spray and hot leg injection. Input air and water flow rates

were monitored and measured by vortex meters and/or turbine meters; location of key flow elements (FE) are identified in Fig. 1. The accuracy of these instruments was better than ±2% of flow. For all test data, temperatures were ambient (~20 to 30°C), and maximum pressures in the test vessel were less than 0.13 MPa (4 psig).

In a typical run, the core spray and/or the hot leg injection water rates were set manually by control valves. The air flow rate was then adjusted by a hand valve to a given value. A series of steady-state data was usually taken at a constant water input rate varying the air flows. For many air/water flow combinations, water was carried out of the hot leg by the air stream. This water was designated as carryover (Fig. 1); whereas, the water that flowed out of the bottom of the test vessel was referred to as fallback. Thus, flow elements were also located in positions to measure the carryover and fallback streams. For conditions of water exiting from the hot leg, the carryover stream was a two-phase mixture (air-water) and was passed through an air-water separator before measuring the single-phase liquid flow. Both the fallback and carryover were returned to the water supply tank.

The test section housing (Fig. 2) was fabricated from 3.8-cm (1.5-in.) thick plexiglass to permit visual observations and photographic studies. Starting at the bottom of the vessel, key components included the air/water mixers for the core spray, rod bundles (grid spacers plus dummy fuel rods), fuel bundle end boxes, upper core support plate (UCSP), and the large upper plenum control rod guide tubes. Air and water core flows entered the test vessel through three mixing devices with one located under each rod bundle. Each mixer consisted of an air and water nozzle; the nozzles were for generating uniform air and water concentrations across the test vessel. Air and water nozzles are identified in Fig. 2. Also, the valving arrangement in Fig. 1 permitted individual control

of air and water flow rates to each nozzle. Water was injected into the hot leg of the test vessel through a 15.2-cm (6-in.) port located 116.8 cm (46 in.) above the upper core support plate; a 20.3-cm (8-in.) port served as the hot leg outlet. For the test data presented, the ports on the narrow sides of the test vessel were employed.

The rod bundles consisted of 16 x 16 arrays of rods (236 dummy fuel rods and 20 dummy control rod guide tubes) in grid spacers. The dummy rods were 1.07 cm (0.422 in.) in diameter, and the dummy control rods were 1.37 cm (0.540 in.) in diameter. Both were 20.3 cm (8 in.) long. This configuration had a length to hydraulic diameter ratio of ∿60. The upper core support plate was simulated with a full-scale model of the support plate above three fuel rod bundles. The large control rod guide tubes were constructed of plexiglass to aid in flow visualization and contained detailed internals including seven baffle plates per tube. Also, the test vessel contained actual reactor hardware from KWU including end boxes, grid spacers, control rod spiders, etc. Thus, the test vessel simulated very accurately a portion (3 out of ∿200 modules) of the upper plenum region of a KWU pressurized water reactor.

INSTRUMENTATION

The measurement of the electrical impedance of a two-phase mixture in the vicinity of a set of electrodes was the basis for operation of the string sensor instrumentation. The electrical conductivity and permittivity of steam or air and water are quite different; thus, as the two-phase flow regime changes at the point of measurement, so does the impedance between probe electrodes. The signal conditioning electronics were designed to convert the measured impedance at the probe to a voltage proportional to that impedance. The output voltage varied from approximately 9 V for air to 100 mV for water (a range of almost 100 to 1). This circuit afforded a high sensitivity in the high void fraction range.

The following relationship between admittance (the inverse of impedance) and void fraction was used to reduce the data in this study:

$$\alpha = \frac{1/Z_f - 1/Z_{mix}}{1/Z_f - 1/Z_g} \quad , \tag{1}$$

where Z_{mix} was the measured mixture impedance. Equation (1) required two calibration points, all water (Z_f) and all air (Z_g), 0 and 1.0 voids respectively.

A two-phase flow velocity can be determined by estimating the transport time of flow perturbations detected by two spatially separated impedance sensors. The transport time was calculated by examining the relative phase shift between two probe signals in the frequency domain. In the frequency domain if two signals are related by a simple time delay, the relative phase shift between signals will be a linear function of frequency, and the slope of this linear function will be equivalent to the transport delay. Thus, the transport time is

$$\tau = \dot{\theta}(f)/360 \quad , \tag{2}$$

and the velocity is then computed by

$$V = D/\tau \quad . \tag{3}$$

The measured impedance by a sensor is obviously a function of the relative amounts of liquid and vapor present and the distribution of those phases, but the measured impedance also depends on the sensor geometry. For application in an upper plenum and to enable flow velocity measurements to be taken, a bi-level string sensor was fabricated (void measurement requires only one sensor level). Figure 3 is a photograph of the string sensor. The probe consisted of a stainless steel frame, 12 x 7 x 2.5 cm, with strut members approximately 0.5-cm thick. The frame held the two levels of electrodes (stainless wire), separated axially by 1.91 cm, in a cross-hatched pattern. The wires were electrically isolated from the frame by maycor inserts. The mixture impedance was sampled by measuring the impedance between adjacent pairs of wires on a sensor level.

A ten-second integration period was used in determining the mixture impedance term, Z_{mix}, in Eq. (1). The average of the void fractions measured by each sensor level was used for all the data presented in this study. The largest difference between voids measured at the two levels was $\pm 3\%$ and most cases the difference was only $\pm 1\%$. A velocity estimate was computed using 100 samples at 2.56 seconds per sample, 256 seconds per estimate. A Hewlett-Packard digital signal analyzer (HP 5420A) was employed to calculate the velocity estimates and an integrating digital voltmeter was used for Z_{mix}.

A gamma densitometer was also located in the test vessel during all tests. The densitometer consisted of a 20 mci Gadolinium 153 (^{153}Gd) gamma source, which was positioned along the vertical centerline of the upper plenum model, a collimated sodium iodide detector (NaI), located outside the lucite wall of the plenum, and associated electronics. The 20-mci ^{153}Gd source was encapsulated near the end of a 2.54-cm (1-in.)-OD stainless steel cylinder, Fig. 1. The NaI detector was operated in the pulse mode with pulse energy acceptance limited to the approximately 100 KeV energy of the ^{153}Gd gamma source. The source and detector position were adjustable along most of the vertical centerline of the test vessel.

The standard equation[8] for attenuation of a gamma beam by two-phase media in series is

$$I = I_o \exp(-\mu \rho_a \ell) \quad , \tag{4}$$

where I_o is the unattenuated beam intensity, μ is the mass absorption coefficient of water, ρ_a is the apparent density, and ℓ is the length of the absorption path. For the single-beam application, the apparent density can be related to the intensity by

$$\rho_a = A \, \ell n \, I/B \tag{5}$$

where the constants A and B can be evaluated from water only and air only calibration data. In the experiments, the readout for the NaI detector was by a scaler-timer and a count ratemeter which monitored current pulses. The rate of current pulses is proportional to intensity and can be used in Eq. (5) for I. Since a good average steady-state density was desired, pulses were totaled for 30 s time intervals, usually taking at least 5 samples (150 s) for each test condition. For this 30 s sampling time, the total counts ranged from ∿90,000 for all air to 10,000 for all water (a range of almost 10). The void fraction is related to the apparent density by,

$$\alpha = \frac{\rho_f - \rho_a}{\rho_f - \rho_g} \quad , \tag{6}$$

where ρ_f and ρ_g are liquid and gas densities, respectively.

A turbo-probe flowmeter (Flow Technology, Inc., Model TR-1) was installed in the upper plenum to measure velocities. The turbo-probe consisted of a turbine flowmeter capsule [2.54-cm-OD (1-in.)] mounted at the end of an insertion probe. The stem of the probe contained an electronic pickoff which sensed the passage of each rotor blade. A pulse output was thus obtained with the repetition rate directly related to flow velocity. The factory calibration data for the flowmeter showed that the output frequency (Hz) varied from ∿60 to 1150 for a flow range of 1.5 to 15 m/s (5 to 50 ft/s).

EXPERIMENTAL RESULTS AND ANALYSIS

A series of 51 steady-state tests were made covering a range of water input rates [0.0019 to 0.0075 m^3/s (30 to 120 gpm)] for both core spray and hot leg injection cases; the air flow rate varied from 0.3 to 1.5 m^3/s (600 to 3200 ft^3/min). For these input flow ranges, the outlet flow conditions spanned from full fallback to total carryover. Also, two special test series were conducted to study instrument location effects in the upper plenum and to extent the range of void fraction measurements. No velocity data were taken for the additional test series. In the text and figures, the volumetric flow rates are presented on the basis of units per test module (three modules in test vessel as shown in Fig. 2); thus, the total volumetric flows are three times greater.

Void Fraction Results

For the main test series, the densitometer source was located 50 cm above the UCSP and at the centerline of the test vessel; the centerline of the string probe was 16 cm from the inside wall of the test vessel (1.8 cm from the vessel centerline) and 18 cm above the UCSP. Void fractions results from the string probe are plotted versus air flow rate in Fig. 5. The trend in the data shows the drying out of the upper plenum with increasing air flow. Water injection point (core spray versus hot leg) and flow rate appear to have little effect on the measured void fraction. Figure 6 is a similar graph with densitometer-determined void fractions plotted against air flow. Again, the drying out of the upper plenum is noted as well as little, if any, effect of water flow rate or injection point on void measurements. A comparison of the void measurements from the densitometer and string sensor is illustrated in Fig. 7. Generally good agreement is shown between $\sim$0.70 and 0.98 void fraction with little scatter. The string probe measured a consistently higher void fraction than did the gamma

densitometer. However, this result was not surprising in that the string sensor monitored flow near the center of the upper plenum, whereas the gamma densitometer void measurement was an average from the centerline of the vessel to the wall. In many flow conditions, water tended to collect on upper plenum surfaces, especially walls; the densitometer apparently sensed this phenomenon but the string sensor did not.

To study the effect of sensor location in the upper plenum a series of tests were conducted. First, the string probe was moved closer to the wall (new position - ℄ 6 cm from wall) as illustrated in Fig. 8. The data presented in Fig. 9 show the effect of moving the string probe. As expected the string sensor measured a much lower void fraction at the new position than near the center of the vessel. The void results as for the previous data appear to be insensitive to water injection rates and exhibit little scatter. In a similar series of tests, the gamma densitometer was repositioned to a height of 30 cm above the UCSP. The effect on void fraction measurements is shown in Fig. 10. The flow in the upper plenum was somewhat stratified, higher density fluid in the vicinity of the UCSP, due to geometry and gravitational effects. Thus, the void fraction results in Fig. 10 are reasonable. Figure 11 is a comparison of the void measurements from the two void monitoring instruments for two string probe locations and a fixed densitometer position. The location effect on string void measurements is obvious and probably corresponds to the collection of water on the walls and UCSP. It is interesting to note that the void fraction from the string sensor was more sensitive to horizontal position than the densitometer results were to vertical location which can be seen by comparing Figs. 9 and 10.

A special test series was run to check the effectiveness of the string sensor instrumentation at lower void fractions ($\alpha < 0.70$). It was necessary to change normal test procedures to achieve low void conditions in the test vessel. For

these cases, the entire vessel was filled with water; air was introduced through one of the outside air nozzles and water flowed through the three core spray nozzles. Under these steady-state conditions extremely good mixing was observed in the vicinity of the UCSP. In this test series the string sensor centerline was 6 cm from the test vessel wall and the gamma source was 30 cm above the UCSP. The void fraction data from the string probe and densitometer are compared in Fig. 12, and excellent agreement is noted for voids ranging from 0.20 to 0.70. For the lowest void test runs ($\alpha < 0.20$) the density stratification was visually much more evident with higher density fluid closer to the UCSP. Since the string sensor was located nearer the UCSP than the densitometer, it follows that the instrument would sense a more dense mixture.

Velocity Measurements

For a typical test run, plots of the coherence function and phase of transfer function are shown in Fig. 13. The coherence function gives an indication of how well flow perturbations sensed by one probe are "seen" by the next. If all perturbations were sensed by both probes, a coherence of one would result. Conversely, if distinctly different signals are measured by both probes, then their coherence would be zero. The slope of the phase curve in Fig. 13 is 2.4 deg/Hz. The transport delay was then calculated from Eq. (2) to be 0.0067 second. The flow velocity computed by Eq. (3) [with D equal 1.91 cm] was 2.9 m/s (9.4 ft/s).

In Fig.14 string probe velocity data are plotted against the air flow rate per module for four water injection rates. As the water flow rate increased, the slope of the curves increased. Also, hot leg injection cases had noticeably lower probe velocities than corresponding core spray points for the highest two water flow rates (30 and 40 gpm). These two flow phenomena may be related, at least in part, to the fact that less air was required to achieve full carryover as input water flow increased.

Turbo-probe velocity results, Fig. 15, tend to fall on a smooth band with increasing scatter as velocities decreased. The turbo-probe was located 18 cm above the UCSP, the same height as the string sensor; the centerline of the meter was 14 cm from the wall. As the air flow increased and the upper plenum dried out, the turbo-probe velocity seemed to approach the air only data.

The string sensor measured the time of flight of flow perturbations to produce a velocity. Thus, at high void fractions, where the liquid phase is discontinuous, the string probe is more sensitive to liquid phenomena. Figure 16 shows a comparison of string probe and turbo-probe velocities. At lower velocity values, both sensors appeared to monitor approximately the same velocity. However, as the velocities increased (and air flow rates increased) the turbo-probe velocity

became much larger than the string probe velocity. This was related to the previous argument that the turbo-probe was more sensitive to air; whereas, the string probe was more influenced by water at high void conditions.

CONCLUSIONS

Air-water testing in an accurate model of a PWR upper plenum region demonstrated that the string probe instrumentation is capable of monitoring two-phase flow. In particular, void fraction measurements obtained by the string sensor agreed very well with an in-situ low energy gamma densitometer over a void range of 0.20 to 0.98. Furthermore, experience suggests that the string probe is sensitive to even much lower void fractions. Flow velocities from the string probe showed reasonable agreement with a turbo-probe at low velocities. However, as velocities increased, the string probe results diverged from the turbo-probe readings. More work is required for interpretation of how string sensor and turbo-probe velocities relate to the two phase flow conditions in the upper plenum region. Several special test series were conducted that highlighted the fact that large density gradients occur in the vicinity of the upper core support plate. More phenomenological flow studies and modeling are needed for a better understanding of two-phase flow in refill and reflood test facilities.

ACKNOWLEDGMENTS

This research was performmed at the Oak Ridge National Laboratory operated by the Union Carbide Corporation for the Department of Energy. This study was part of the Advanced Instrumentation for Reflood Studies (Manager - P. G. Smith) and Instrument Development Loop (Manager - D. G. Thomas) Programs under the sponsorship of the U.S. Nuclear Regulatory Commission. The authors wish to acknowledge Roy Shipp, Jr. for the development of the low energy gamma densitometer and assistance of P. H. Hayes and W. H. Glover in performing the experiments.

NOMENCLATURE

A,B	Constants in Eq. (5)
D	Distance between string sensor levels
I	Attenuated gamma beam intensity
I_o	Unattenuated gamma beam intensity
ℓ	Length of absorption path
Z	Impedance
α	Void fraction
μ	Mass absorption coefficient
ρ	Density
τ	Transport time
$\dot{\theta}$	Gradient of phase curve

Subscripts

a	Apparent
f	Fluid (water)
g	Gas (air)
mix	Two-phase mixture

LIST OF FIGURES

REFERENCES

1 Hewitt, G. F., "The Role of Experiments in Two-Phase Flow Systems with Particular Reference to Measurement Techniques," Progress in Heat and Mass Transfer, Vol. 6, 1972, pp. 295-324.

2 Aya, I., "A Model to Calculate Mass Flow Rate and Other Quantities of Two-Phase Flow in a Pipe with a Densitometer, a Drag Disk, and a Turbine Meter," ORNL/TM-4759, Nov. 1975, Oak Ridge National Laboratory, TN.

3 Banerjee, S., et al., "Measurement of Void Fraction and Mass Velocity in Transient Two-Phase Flow," Proceedings of the CCNI Specialists Meeting, Toronto, Canada, Vol. 2, Aug. 3-4, 1976, pp. 789-832.

4 Eads, B. G., et al., "Advanced Instrumentation for Reflood Studies Program Quarterly Progress Report, October 1-December 31, 1977," ORNL/NUREG/TM-202, Sept. 1978, Oak Ridge National Laboratory, TN.

5 Aerojet Nuclear Company, "Developments of Instruments for Two-Phase Flow Measurements," ANCR-1181 1974, Idaho Falls, Idaho.

6 Oak Ridge National Laboratory 1976, "Project Description of ORNL PWR Blowdown Heat Transfer Separate Effects Program Thermal-Hydraulic Test Facility (THTF)," ORNL/NUREG/TM-2, Feb. 1976, Oak Ridge National Laboratory, TN.

7 Carrard, G. and Ledwidge, T. J., "Measurement of Slip Distribution and Average Void Fraction in an Air-Water Mixture," Proceedings of the International Symposium on Two-Phase Systems, Vol. 6, Progress in Heat and Mass Transfer," Haifa, 1971, Pergamon Press (1972).

8 Rockwell, T., ed., Reactor Shielding Design Manual, Van Nostrand, New York, 1956.

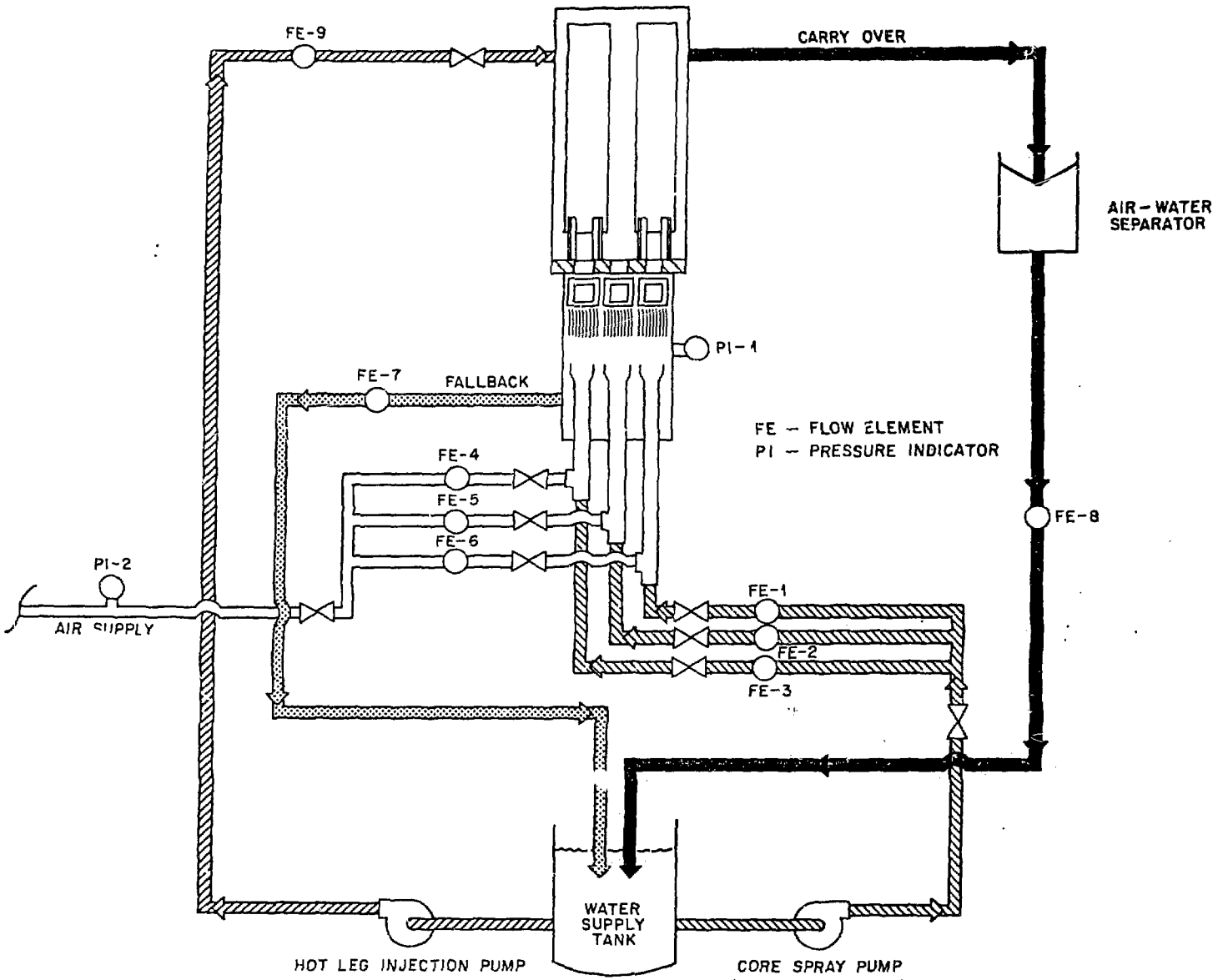

Fig. 1 Flow schematic of the test facility.

ORNL-DWG 79-6062 ETD

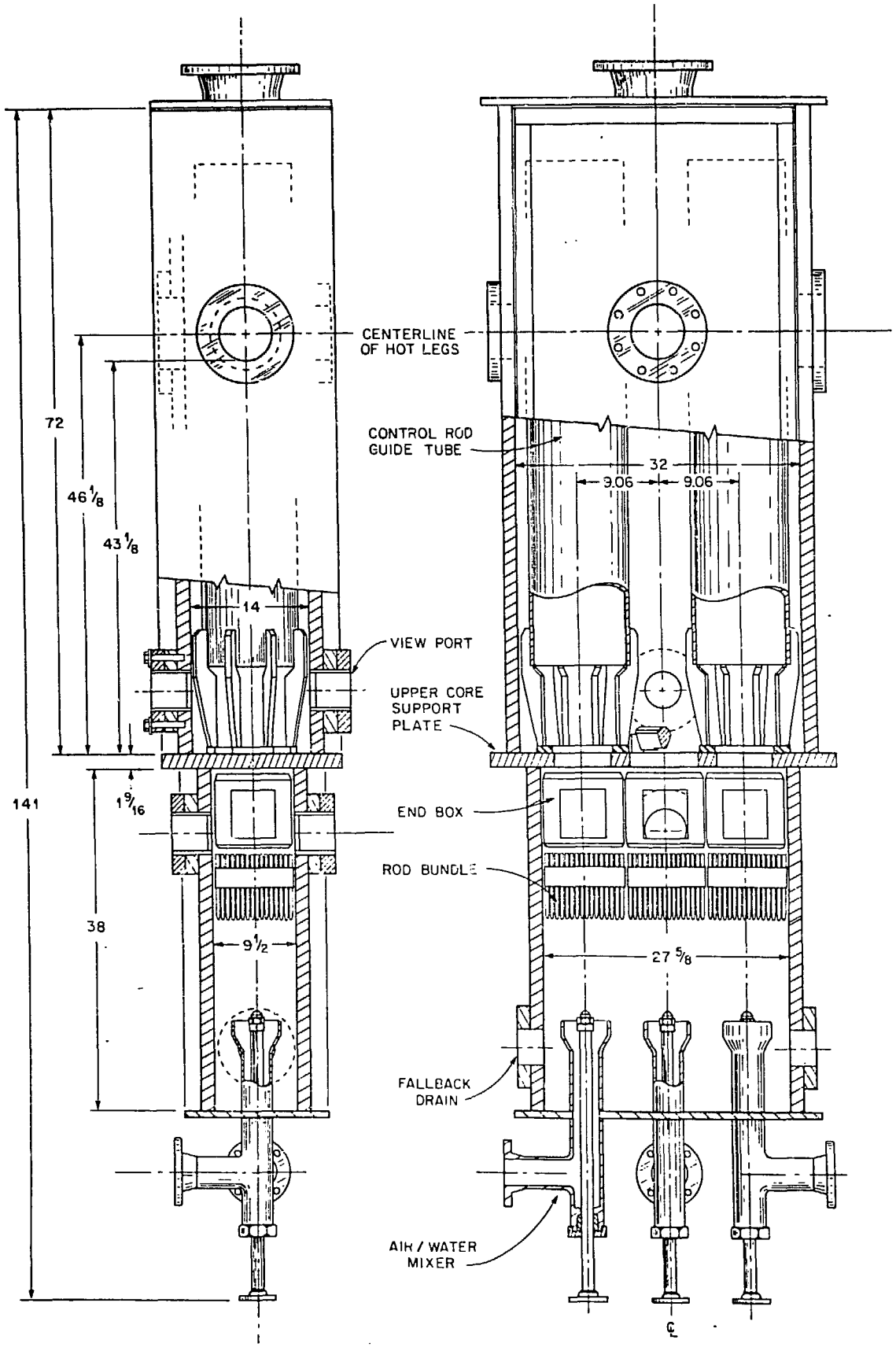

Fig. 2 Details of the test vessel.

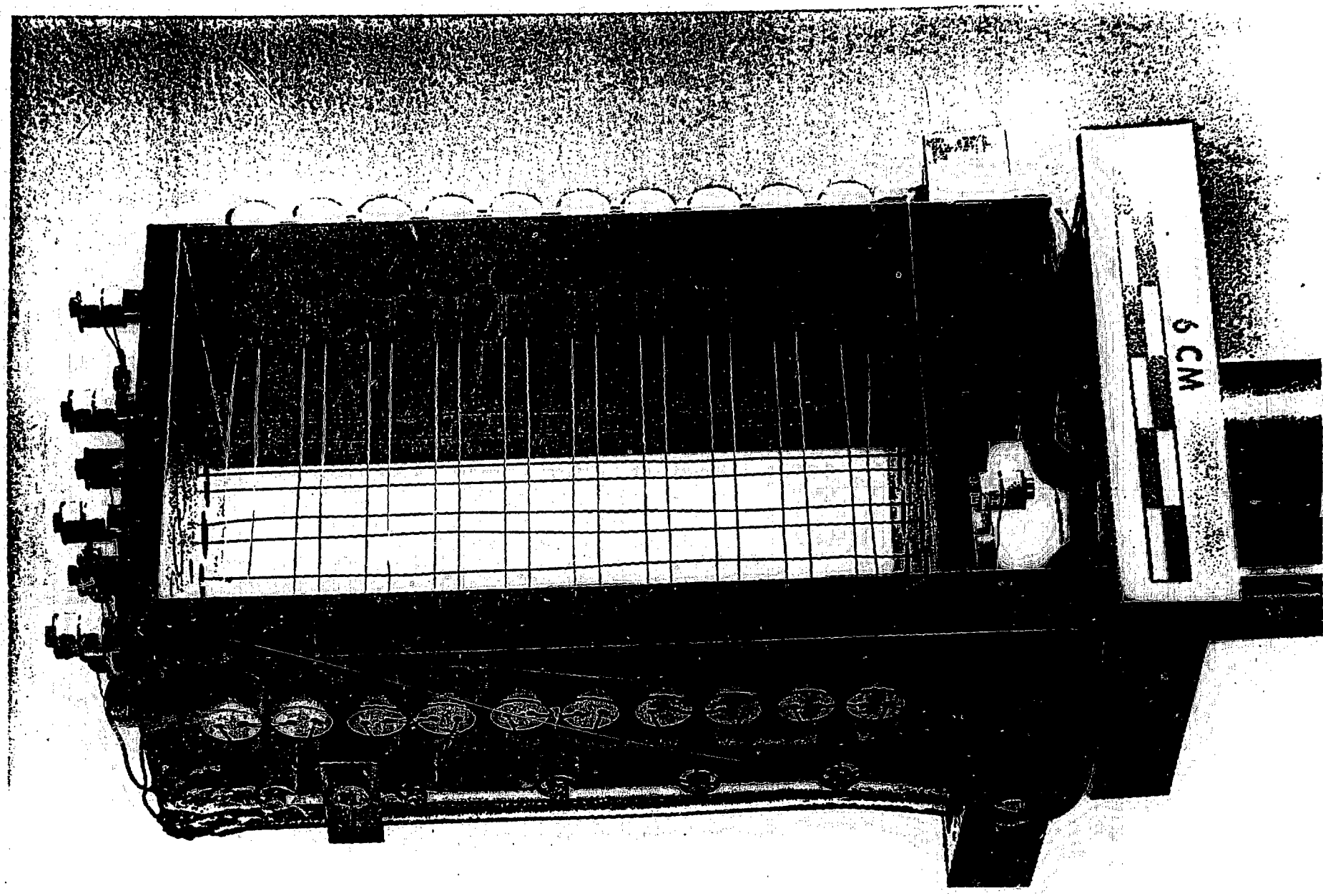

Fig. 3 Photograph of upper plenum string sensor.

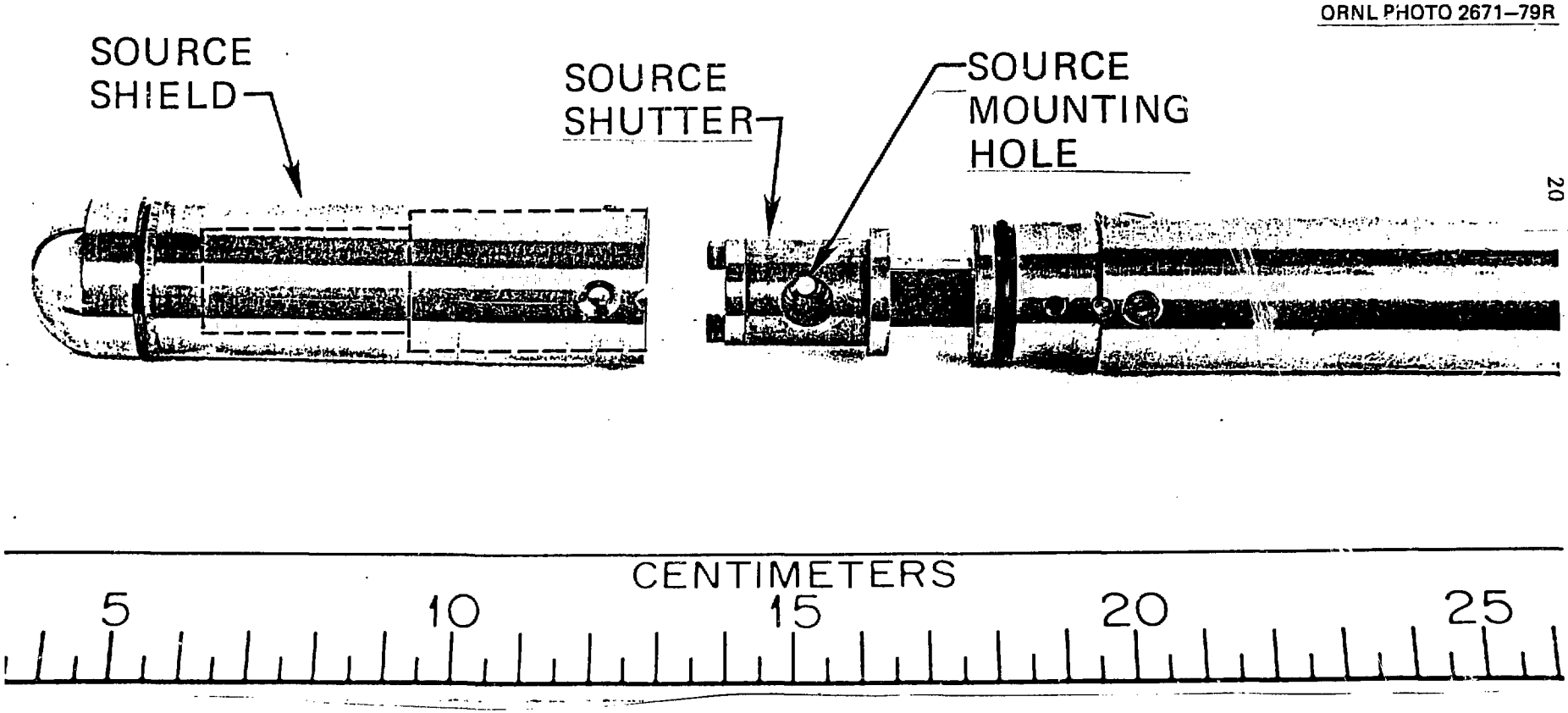

Fig. 4 Photograph of source capsule for low energy gamma densitometer.

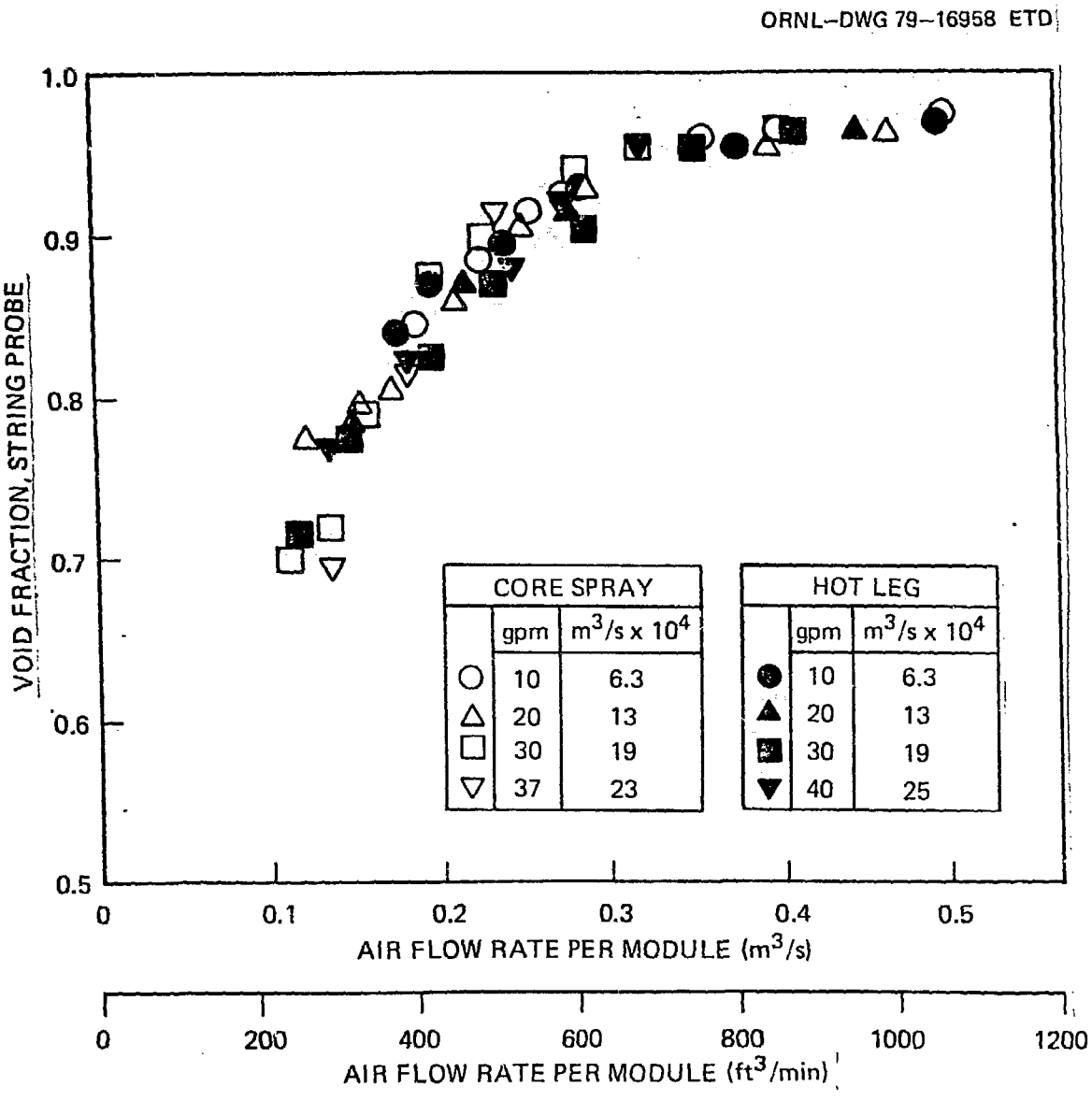

Fig. 5 String probe void fraction versus air flow rate.

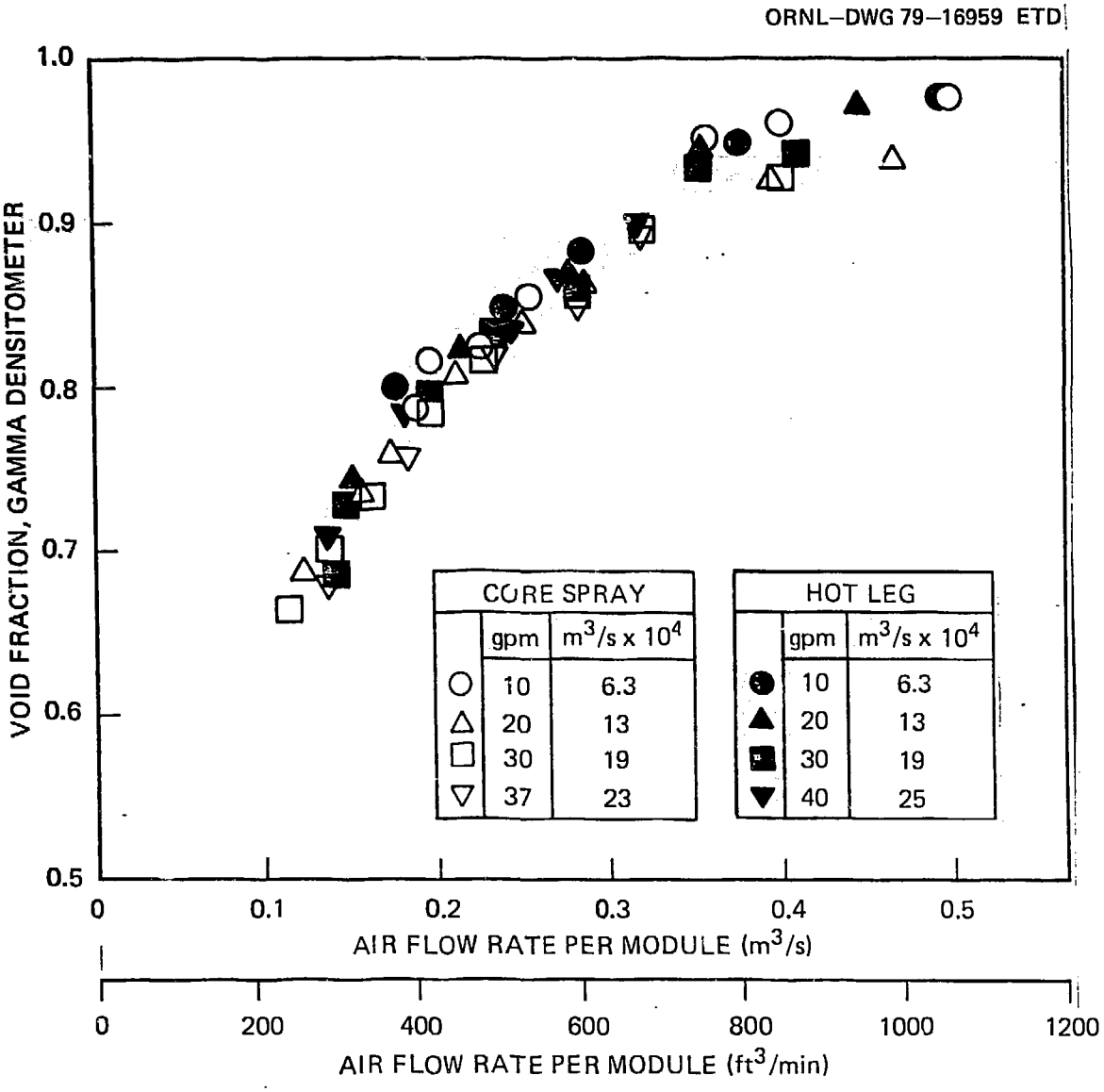

Fig. 6 Gamma densitometer void fraction versus air flow rate.

ORNL–DWG 79–16957 ETD

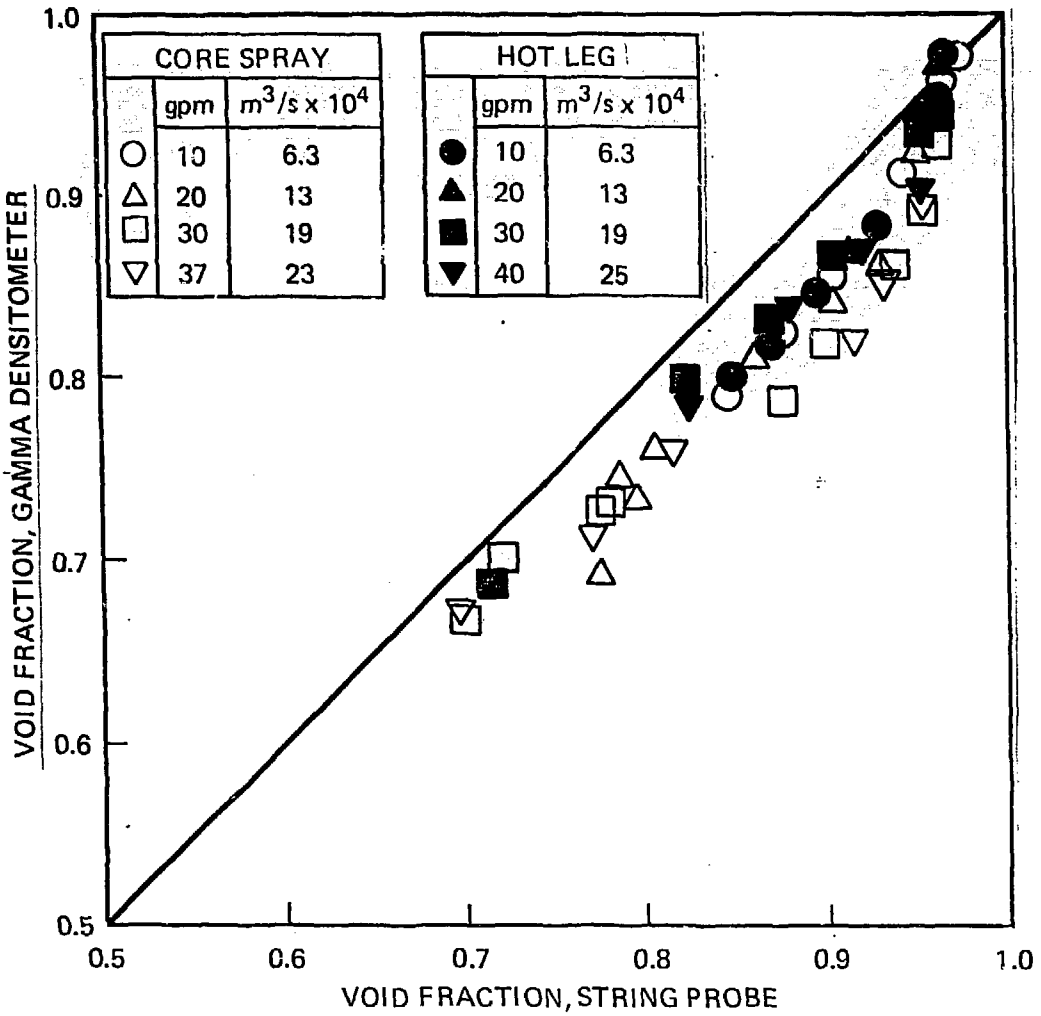

Fig. 7 Comparison of void fractions determined by string probe with those from gamma densitometer.

File as original

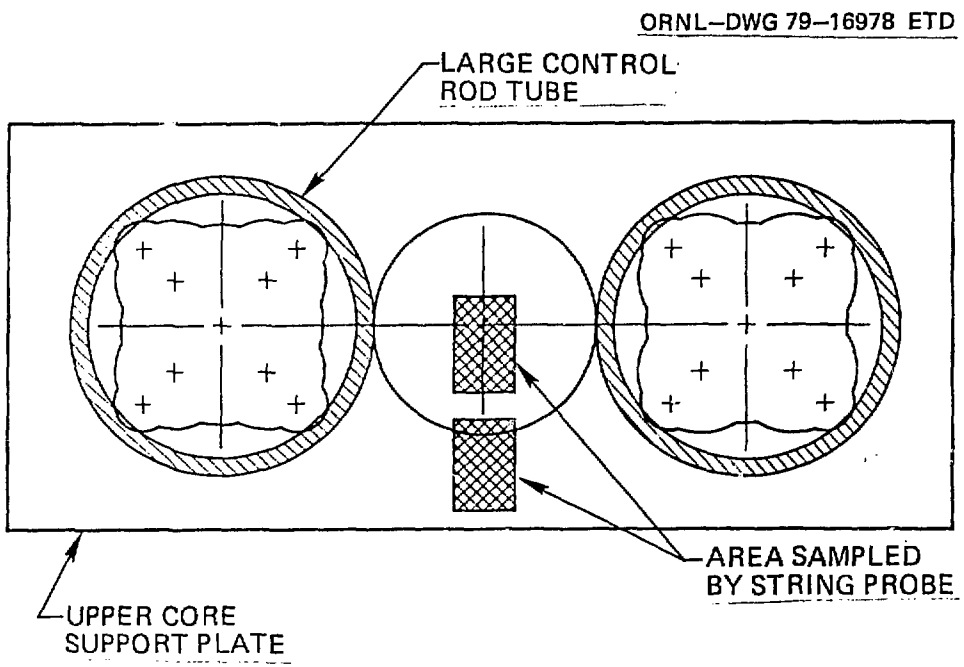

Fig. 8 Relative positions of string probe above upper core support plate.

combs

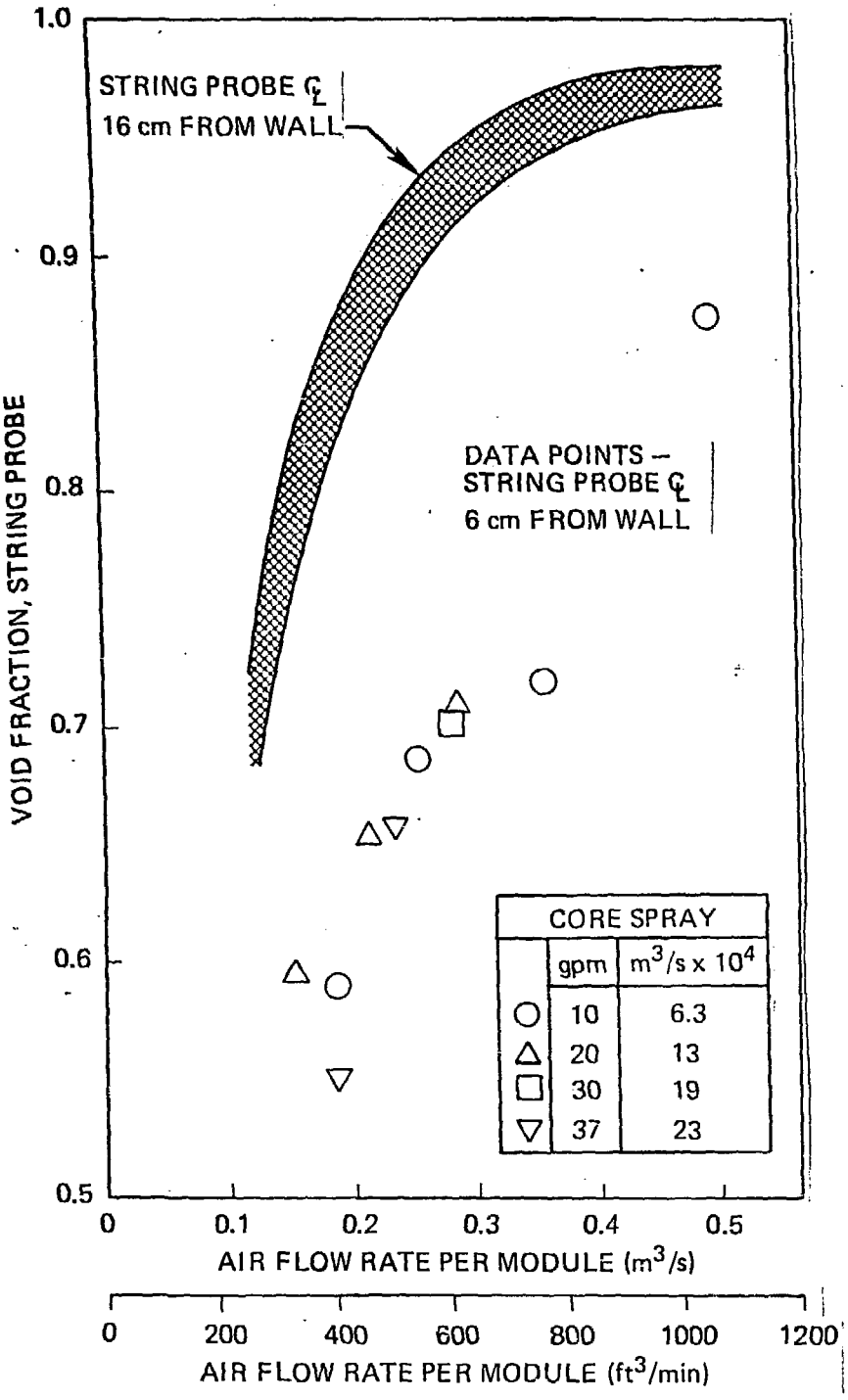

Fig. 9 Effect of string probe location on void fraction measurements.

ORNL–DWG 79–16956 ETD

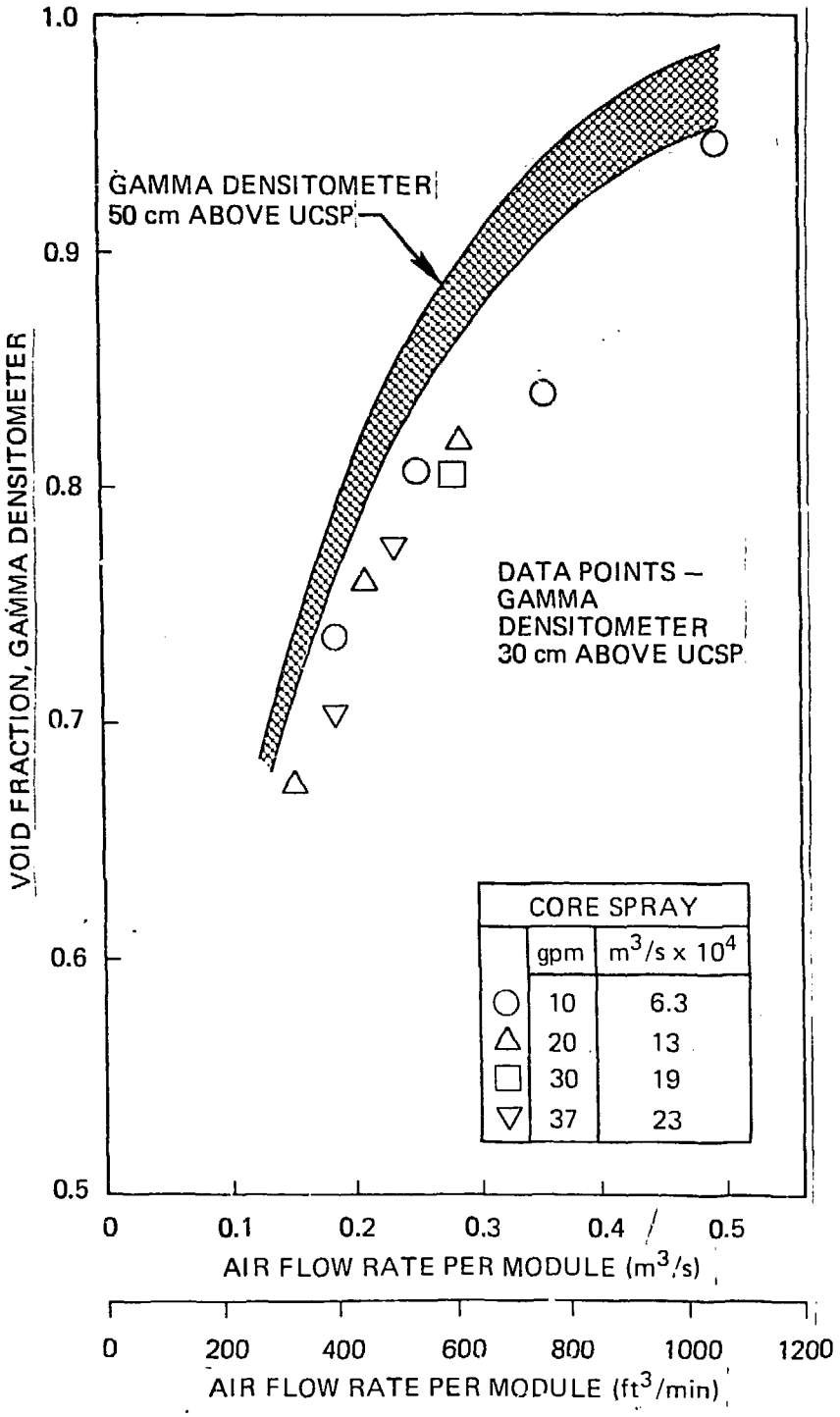

Fig. 10 Effect of densitometer vertical location on void fraction measurements.

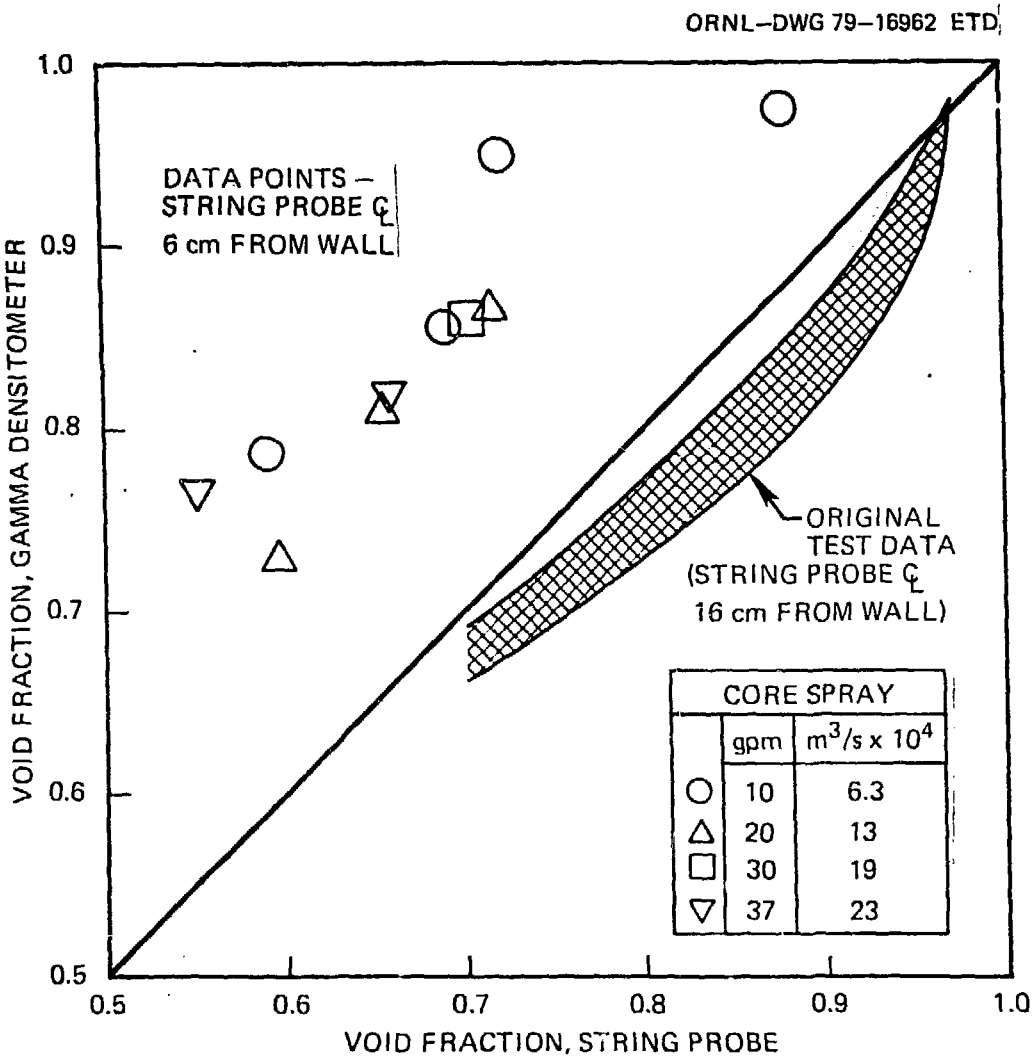

Fig. 11 Comparison of void measurements from string probe to densitometer for different string sensor locations with a fixed densitometer location (50 cm above UCSP).

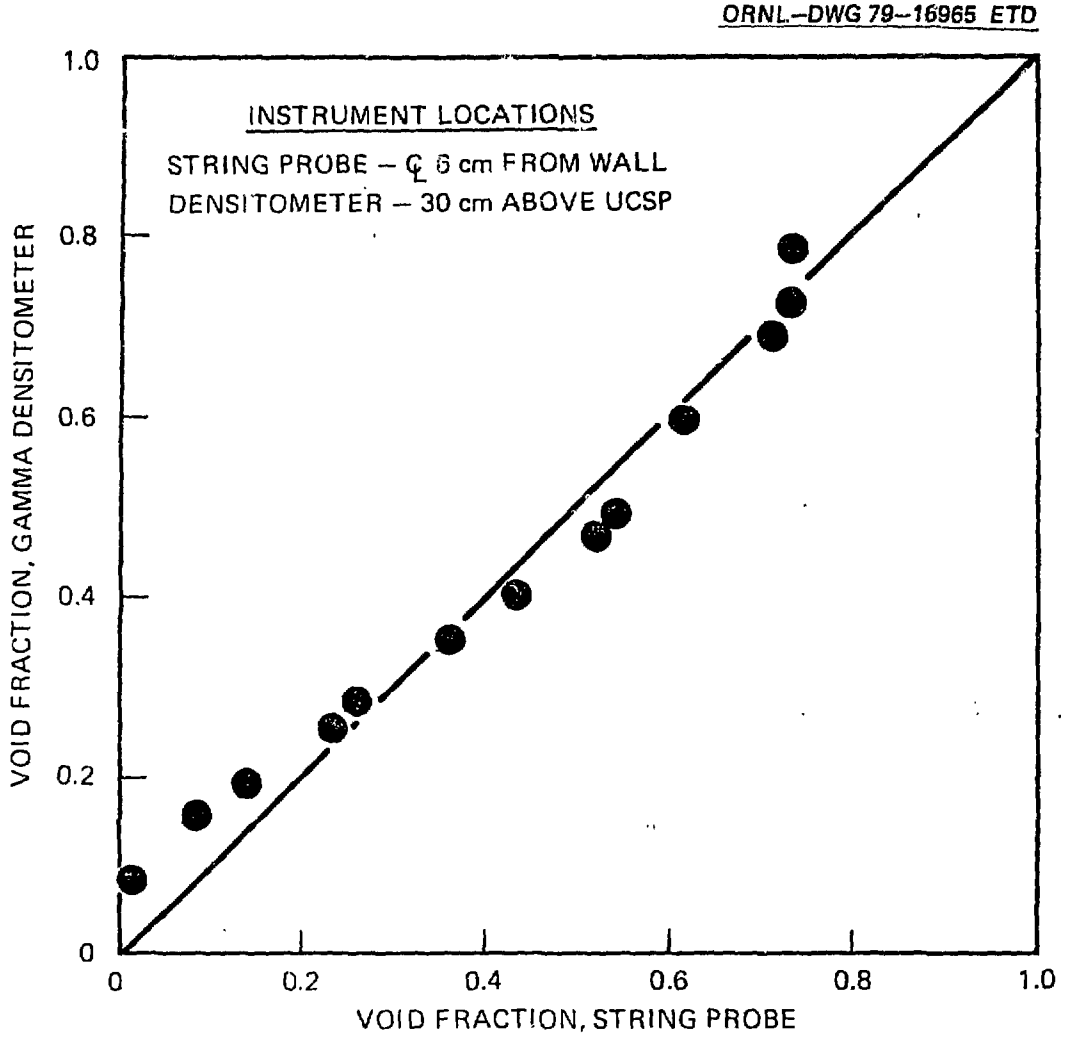

Fig. 12 Results of special tests including low void fraction data.

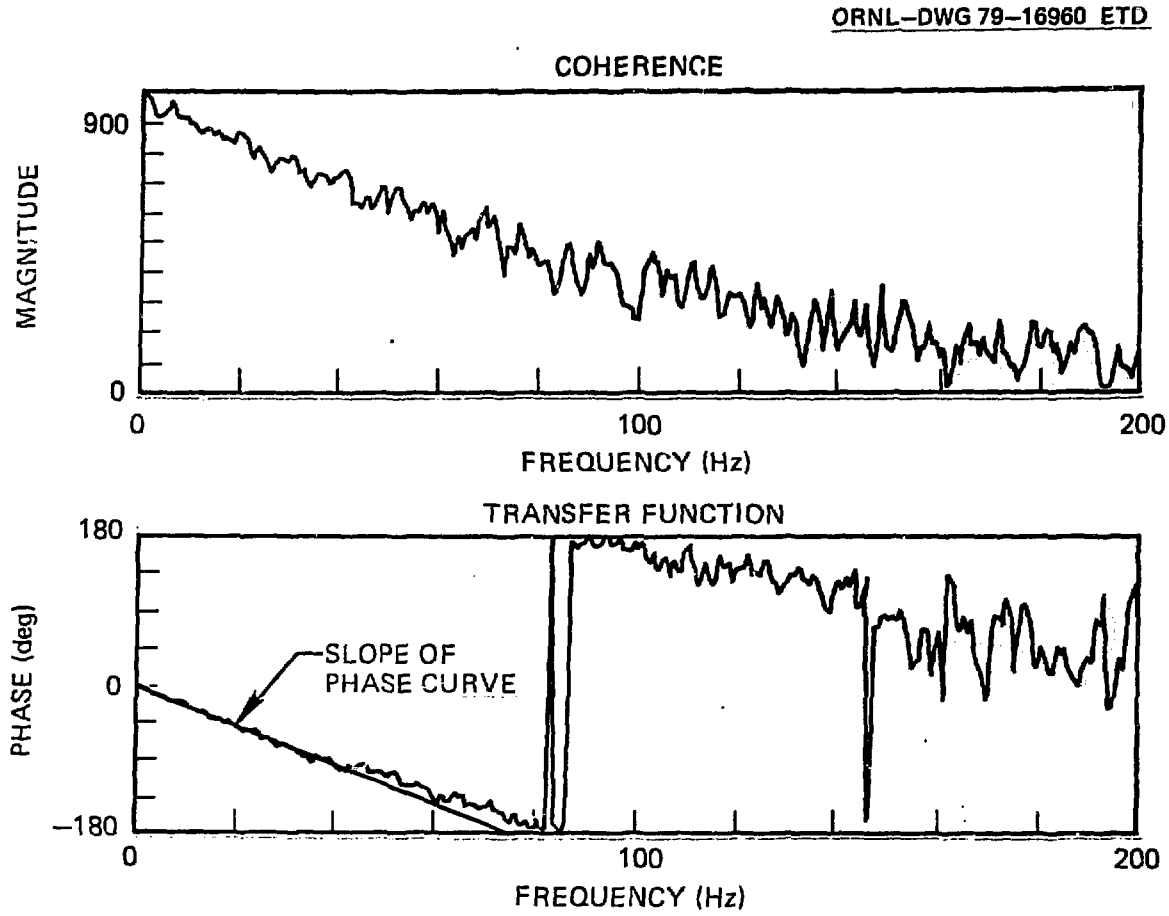

Fig. 13 Coherence and phase plots for a typical test condition.

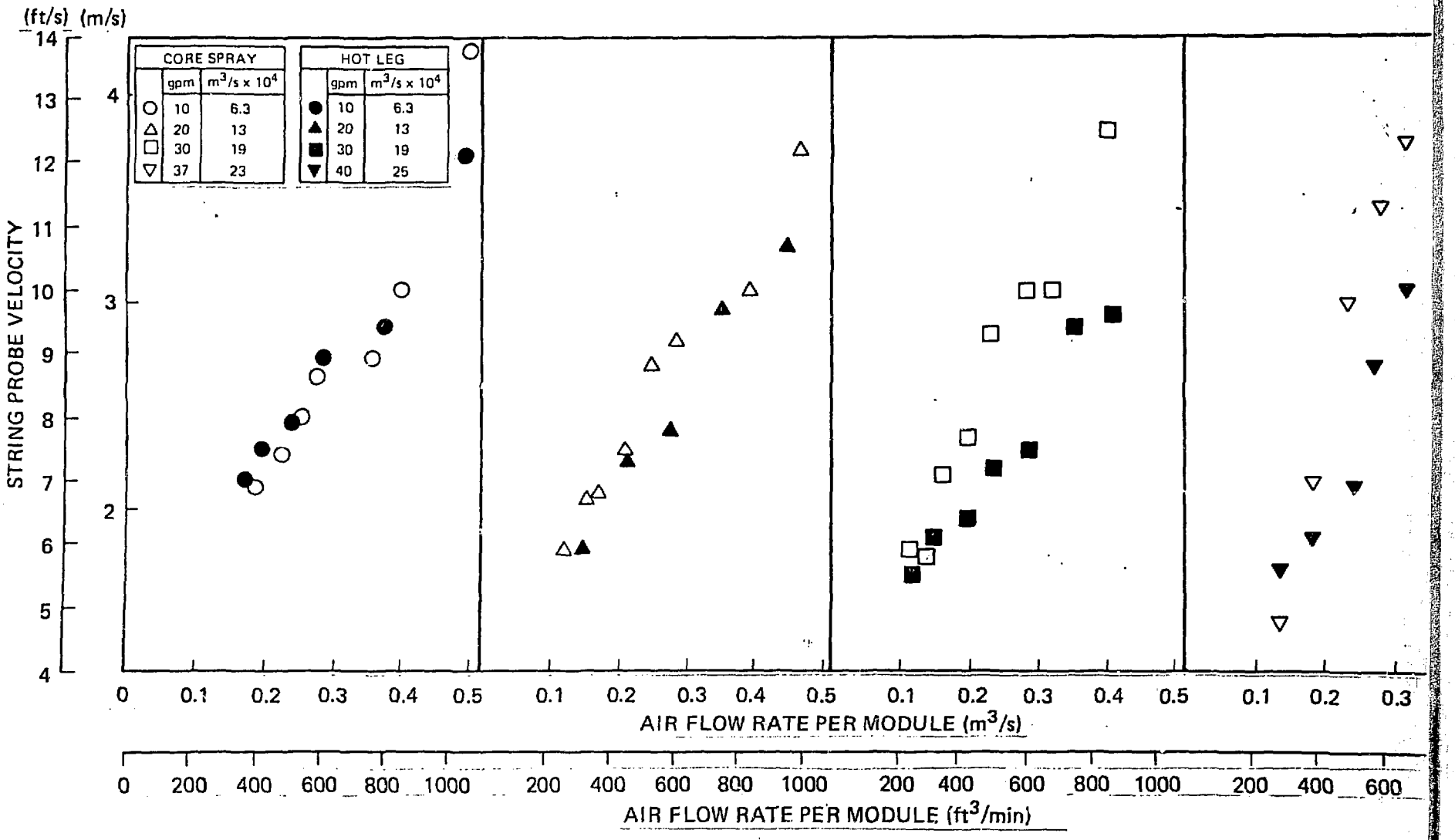

Fig 14 String probe velocity versus air flow rate.

ORNL–DWG 79–16963 ETD

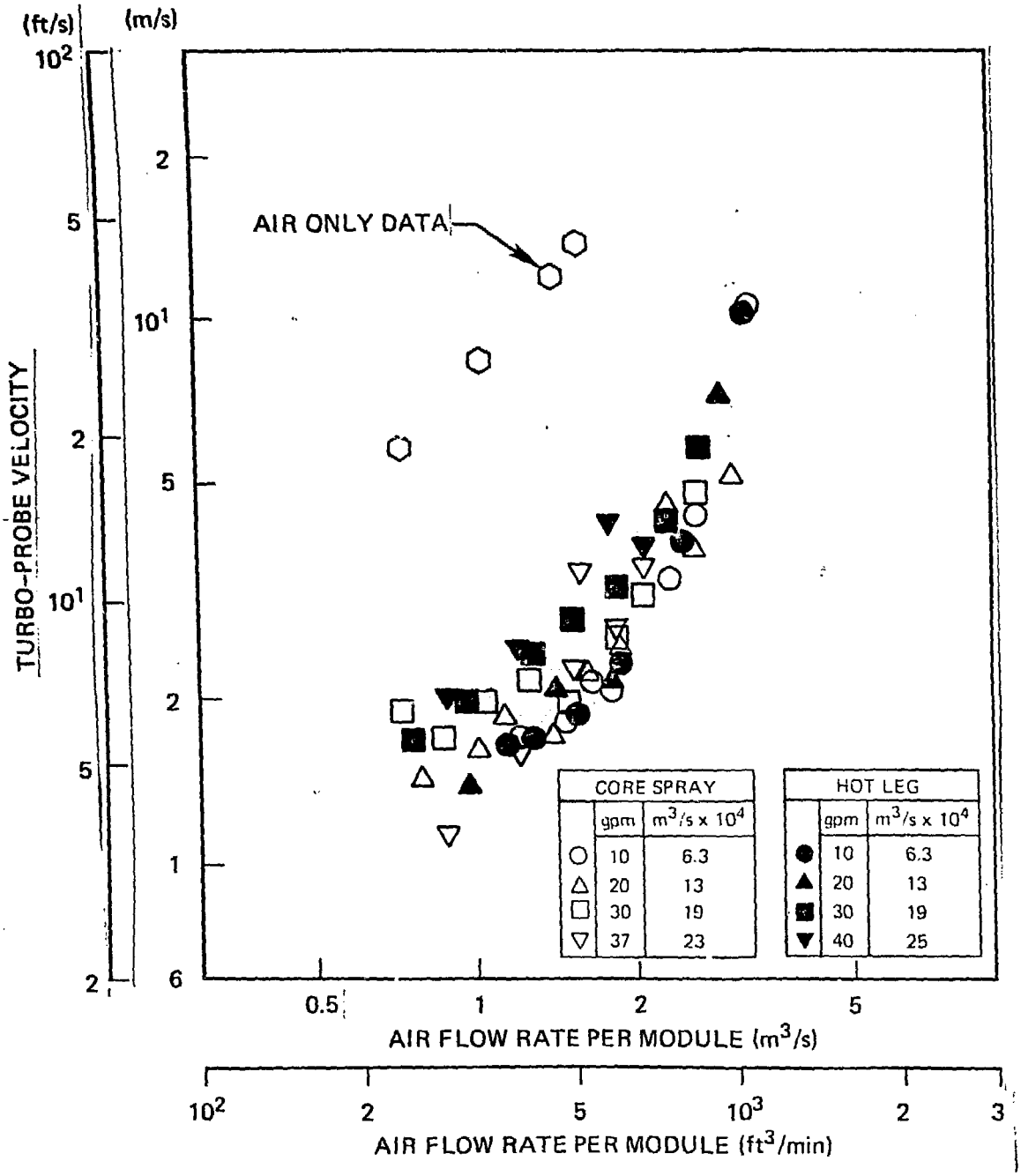

Fig. 15 Turbo-probe velocity versus air flow rate.

ORNL–DWG 79–16964 ETD

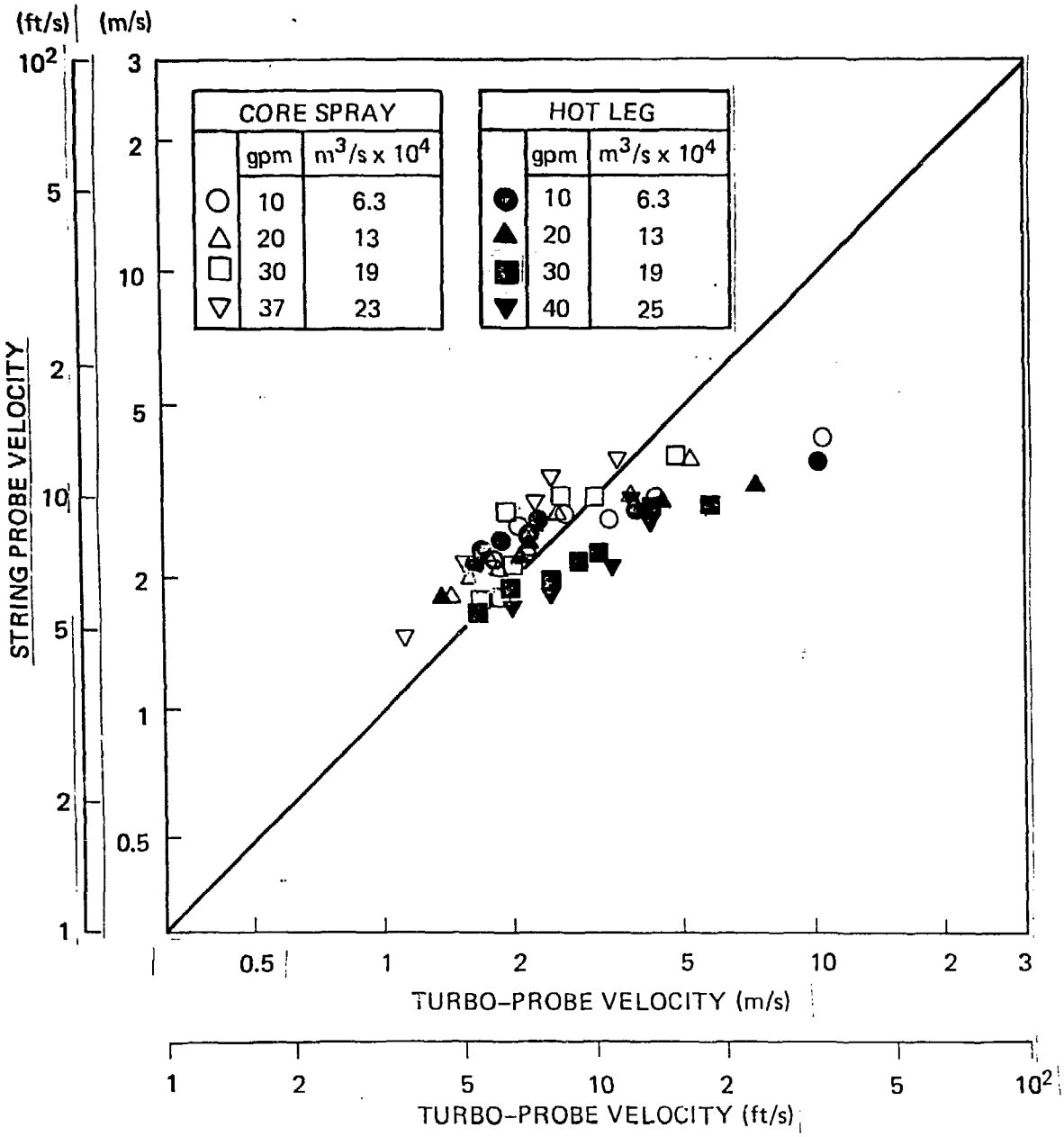

Fig. 16 Comparison of velocities from string probe with those from turbo-probe.